

POLARIZATION AT THE EXTREME LIMB OF THE SUN AND THE ROLE OF ECLIPSE OBSERVATIONS

JAN O. STENFLO

*Institute of Astronomy, ETH Zentrum, CH-8092 Zurich, and
Faculty of Mathematics & Science, University of Zurich*

Abstract. Scattering of light in the Sun's atmosphere produces polarization throughout the solar spectrum. Due to the changing scattering geometry this polarization increases monotonically from disk center towards the solar limb. Many different factors influence the magnitude of the polarization: The intrinsic polarizability of the scattering atomic system (combination of angular momenta and nuclear spin for the involved atomic levels, quantum interferences and optical pumping), collisional processes and depolarizing magnetic fields, the ratio between line and continuum opacities, anisotropies of the radiation field, small-scale structuring of the atmosphere (deviations from plane-parallel stratification), etc. As all these effects vary greatly from line to line, the linearly polarized spectrum becomes richly structured, in a way that has little resemblance to the structuring of the intensity spectrum. According to a classic solution by Chandrasekhar for an idealized, purely scattering plane-parallel atmosphere the linear polarization reaches asymptotically at the extreme limb the very high value of 11.7%. Measurements a few arcsec inside the limb show much smaller polarization values, generally much below 1%, and in most cases less than 0.1%. The polarization amplitude is however expected to increase dramatically at the extreme limb, within the last arcsec, and could possibly approach the Chandrasekhar limit in some spectral lines. Observations of this increase have not been possible in the past due to seeing effects in the Earth's atmosphere, telescope resolution, and stray light in the instrument. All these limitations can be avoided at a total solar eclipse, when the edge of the Moon is used as a knife edge to isolate the extreme limb from the glaring radiation of the solar disk, to allow us to record the polarization from the separate height layers of the atmosphere, from the photosphere through the chromosphere. This has to be done during the brief flash phase of the eclipse (the transition to totality at second contact, or the emergence from totality at third contact). The polarization of the flash spectrum has never been successfully recorded in the past but is being done by a Swiss team from ETH Zurich during the 29 March 2006 eclipse at Waw an Namos, Libya.

Key words: polarization, coherent scattering, solar eclipse, flash spectrum

1. Introduction

Due to coherent light scattering in the Sun's atmosphere the solar spectrum gets linearly polarized, even in the absence of any magnetic fields. In recent years it has been found that this linearly polarized spectrum is as richly structured as the ordinary intensity spectrum, but that the spectral structures are very different and governed by other physical processes than those of the ordinary intensity spectrum (Stenflo, 2004). Since we are dealing with a very different and previously unfamiliar spectrum, the linearly polarized spectrum is referred to as the "Second Solar Spectrum" (Stenflo & Keller, 1996; Stenflo & Keller, 1997). The amplitude of the scattering polarization is found to increase steeply as we approach the solar limb.

In radiative-transfer theory there is a classic analytical solution by Chandrasekhar (1950) for an ideal, purely scattering, plane-parallel atmosphere, which shows how the polarization amplitude increases to asymptotically 11.7% at the very edge of the Sun's limb. Although this idealized treatment gives us general guidance, the real Sun differs in various ways. The real atmosphere is far from purely scattering, since collisional effects (collisional excitation, deexcitation, broadening, and depolarization) and competing, non-polarizing opacity sources play a significant role, and these effects are height dependent. The various Fraunhofer lines are formed at different heights in the atmosphere. The position of the limb depends on wavelength. For photospheric spectral lines the limb lies below the chromosphere. The structure of the chromosphere at the

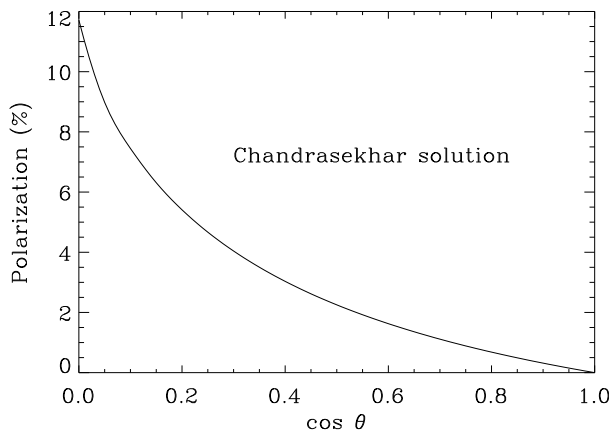


Fig. 1. Degree of linear polarization produced by an idealized plane-parallel atmosphere, in which the radiative transfer is governed exclusively by classical dipole-type scattering (like Thomson scattering at free electrons). The plane of polarization is oriented perpendicular to the radius vector (the line from disk center to the chosen disk position). The center-to-limb distance is given in terms of $\mu = \cos \theta$, where θ is the angle between the vertical direction and the line of sight (the heliocentric angle). The polarization increases from zero at disk center ($\mu = 1$) to 11.7% at the extreme limb ($\mu = 0$).

limb is characterized by a forest of spicules (plasma jets that shoot out from below), which means that the plane-parallel concept becomes meaningless. We thus see that the way in which the scattering polarization varies asymptotically near the extreme limb depends on the height and physics of the line formation process, which is individual for each spectral line considered, and it also depends on the microstructuring of the solar chromosphere.

At second contact during a total solar eclipse we have a transition to totality, when the Moon covers up the last sliver of the Sun's disk. As the Moon moves about $\frac{1}{2}$ arcsec per second (360 km/s on the Sun), the flash phase only lasts on the order of 10 s. During this brief time the Sun's spectrum changes dramatically, from the usual absorption-line spectrum to an emission spectrum, since the continuous spectrum vanishes in the chromosphere, and only the strong chromospheric resonance lines stand out in emission, together with the coronal forbidden lines. With an experiment for the 29 March 2006 eclipse at Waw an Namos, Libya, we (Feller *et al.*, 2006) aim to capture the polarization of this emission line spectrum over the whole visible spectral range, from the UV to the near IR, with high time resolution (about 50 frames per second), which corresponds to the phenomenal height resolution on the Sun of about 10 km.

2. Polarization of the continuum

Real stellar atmospheres behave very differently from the idealized Chandrasekhar case, since many different competing opacity sources contribute to the formation of the spectrum, and the relative weights of the various contributions are strongly height dependent. The dominating opacity source for the Sun's continuous spectrum in the visible range is H^- , which acts as pure absorption and does not generate any polarization. All the polarization of the continuum can be attributed to two processes: (1) Rayleigh scattering at neutral hydrogen, and (2) Thomson scattering at free electrons. Both processes behave like classical dipole scattering.

The physics behind the formation of the Sun's visible continuum is almost exclusively determined by the interaction between radiation and hydrogen plus free electrons. The contributions from other chemical elements are insignificant. Figure 2 from Stenflo (2005) gives an overview of the opacity sources between 3000 and 7000 Å. As the relative

POLARIZATION AT THE EXTREME LIMB OF THE SUN

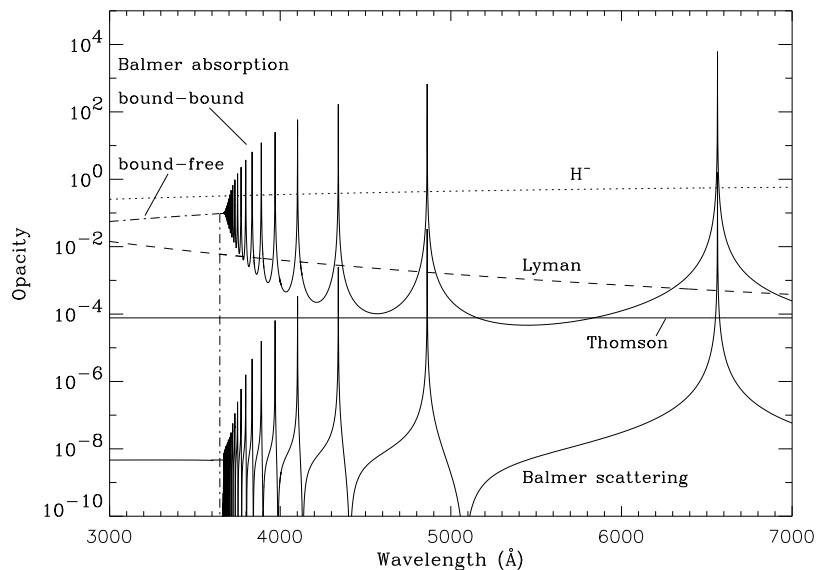


Fig. 2. Opacity contributions (in arbitrary units) to the visible part of the Sun's continuous spectrum, from Stenflo (2005). The diagram is representative of the temperature-density conditions at a height in the solar atmosphere where the Sun's spectrum at a disk position of $\mu = 0.1$ is predominantly formed.

magnitudes of the various opacity sources depend on temperature and density, this type of diagram is strongly height dependent. Figure 2 is representative for the heights in the solar atmosphere, where the spectrum at a disk position of $\mu = 0.1$ (about 5 arcsec inside the limb) is formed.

The vast majority of the neutral hydrogen atoms are in the ground state. Resonant transitions from the ground state would result in the EUV lines of the Lyman series, but for photons at visible wavelengths we are far from these resonances. Still scattering from the ground state can be viewed as scattering in the Lyman series lines, although in the distant line wings. Since the scattering probability in the dispersion wings drops off fairly slowly, as $\Delta\lambda^{-2}$, with distance from the respective resonances, this Rayleigh scattering (labeled "Lyman" in Fig. 2) is still very significant at visible wavelengths and the second most important opacity source after H^- absorption.

A competing opacity in the visible is provided by the bound-bound transitions in the Balmer series (that start from the second, excited level in hydrogen, with $n = 2$, which however is orders of magnitude less populated than the ground state, due to the Boltzmann factor). Due to the increasing Stark broadening of these transitions from random electric fields as we approach the series limit, they merge and converge into a quasi-continuum well before the nominal series limit (at 3646 Å) is reached. As we approach the series limit this non-polarizing bound-bound opacity overtakes the polarizing Lyman scattering opacity, which leads to an effective Balmer jump in the degree of linear polarization before the series limit is reached.

Only a small fraction of the bound-bound absorption transitions represent scattering (spontaneous emission back to level $n = 2$ after the radiative absorption from level $n = 2$), but this opacity source can be neglected in comparison with the others, except near the center of each Balmer resonance.

Figure 3, from Stenflo (2005), illustrates how the polarization of the Sun's continuum varies with wavelength and μ (representing the center-to-limb distance). The left panels give the polarization in log scale, the right panels in linear scale. The wavelength dependence, given in the top panels for $\mu = 0.1$, shows a steep increase in the polarization as we go to shorter wavelengths. This increase has two sources: (a) The limb

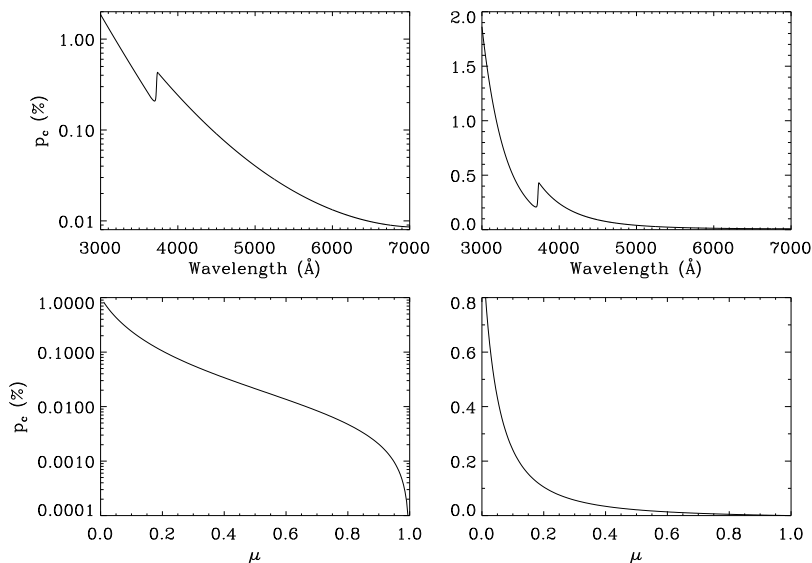


Fig. 3. Linear polarization of the Sun’s continuous spectrum as a function of wavelength (top panels) and center-to-limb distance as parametrized by μ (bottom panels), from Stenflo (2005). The top panels are empirical determinations for $\mu = 0.1$, based on the Atlas of the Second Solar Spectrum (Gandorfer, 2000, 2002, 2005), while the bottom panels are for a wavelength of 4000 Å and based on a scaled version of the theoretical results of Fluri & Stenflo (1999).

darkening, being the source of the anisotropy of the radiation field, increases strongly with decreasing wavelength. The polarization scales with the degree of anisotropy. (b) The ratio between the polarizing Lyman scattering opacity and the non-polarizing H^- opacity increases with decreasing wavelength. The Balmer jump, which lies about 100 Å redwards of the nominal series limit due to the merging of the crowded bound-bound transitions, is produced when the non-polarizing Balmer absorption becomes larger than the Lyman scattering opacity (cf. Fig. 2).

The wavelength dependence in the two top panels is not based on any theory but is entirely empirical. It has been extracted from Gandorfer’s Atlas of the Second Solar Spectrum (Gandorfer, 2000, 2002, 2005) through an elaborate reduction procedure (cf. Stenflo, 2005). The center-to-limb variation in the two bottom panels is however based on the radiative-transfer theory of Fluri & Stenflo (1999), scaled to make the $\mu = 0.1$ amplitude agree with the empirically determined values.

The center-to-limb variation, given in the bottom panels for a wavelength of 4000 Å, differs considerably from the corresponding Chandrasekhar solution in Fig. 1, in two main respects: (1) The center-to-limb variation of the continuum polarization is much steeper. (2) The polarization amplitudes are much smaller, by an order of magnitude near the limb, and much more at larger limb distances. There are several reasons for this difference: The limb darkening for a purely scattering atmosphere is very different from that of the Sun’s atmosphere, which is strongly wavelength dependent. The ratio between the polarizing scattering opacity and the non-polarizing H^- opacity is of order 0.1 (although wavelength dependent) and varies with height. This ratio decreases with increasing depth in the atmosphere. Since we for larger μ look deeper into the atmosphere, below the main scattering layer, the polarization decreases faster with increasing μ than for the Chandrasekhar solution.

Not only the continuum but also the polarization inside resonance lines is found to exhibit a similar qualitative behavior, with a much steeper center-to-limb variation than the Chandrasekhar solution. The expected line polarization is determined largely by the height variation of the radiation-field anisotropy on the one hand (governed by

radiative-transfer physics) and the intrinsic polarizability of the line transitions on the other hand (governed by the quantum structure of the scattering system).

3. Quantum physics and intrinsic polarization

The intrinsic polarizability of a scattering transition generally depends on the total angular momenta of the atomic levels that are involved in the scattering event. The polarizability can be characterized by the parameter W_2 , which is the fraction of scattering events that behave like classical dipole scattering. The remaining fraction, $1 - W_2$, then behaves like isotropic, unpolarized scattering. Usually it is the J quantum numbers of the initial, intermediate, and final levels that are relevant, but in systems with non-zero nuclear spin I , this spin couples with J to form a new total angular momentum quantum number F , which then becomes the relevant one. However, these quantum numbers are only part of the story: the intrinsic polarizability can be drastically altered by quantum interferences between the atomic levels as well as by polarization transfers through optical pumping.

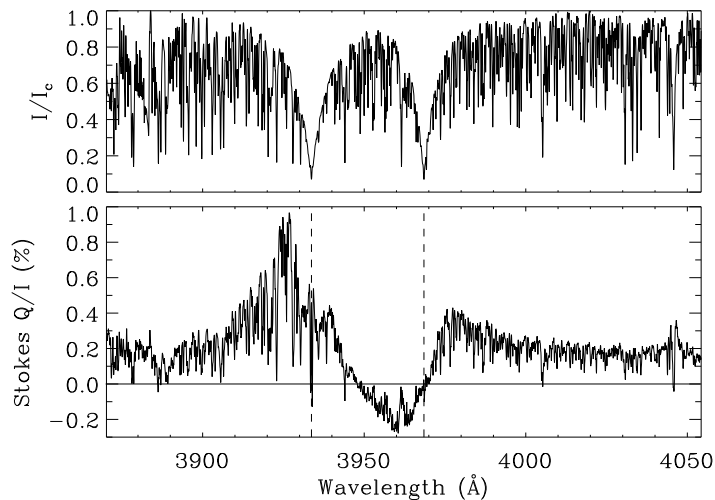


Fig. 4. Illustration of quantum interference in the Ca II K and H line transition system. The recording of the intensity (top panel) and degree of linear polarization (Stokes Q/I , bottom panel) over a range of 180 Å at disk position $\mu = 0.14$ was obtained in 1978 at the Kitt Peak Observatory (Stenflo, 1980). The dashed vertical lines in the bottom panel mark the wavelengths of the K and H line resonances.

Figure 4 illustrates the effect of quantum interference between atomic states with different J quantum numbers. The top panel shows the intensity spectrum covering a range of 180 Å around the K and H lines of singly ionized calcium (Ca II 3933 and 3968 Å, respectively), while the bottom panel gives the simultaneously recorded degree of linear polarization. The recording was made with the spectrograph slit placed 10 arcsec inside the solar limb (Stenflo, 1980). The myriad of spectral structures that we see are not due to noise but to the large number of blend lines in this spectral region. Here we focus our attention on the large-scale envelop variation, which is due to the Ca II K and H system. We notice that the polarization is highly asymmetric around the K line, becomes negative (meaning that the plane of polarization is perpendicular to the solar limb) for a long stretch between the two lines, and then has a zero-crossing at the center of the H line resonance. This strange behavior is governed by quantum interference.

The K and H line transitions have a common ground state, with $J = \frac{1}{2}$, while for the excited state $J = \frac{3}{2}$ for the K line and $\frac{1}{2}$ for the H line. With this quantum number combination the H line should be intrinsically unpolarizable ($W_2 = 0$), while the K line should have $W_2 = \frac{1}{2}$. The two transitions are however not independent of each other.

When the calcium ion is radiatively excited, it does not choose between the $J = \frac{3}{2}$ and $\frac{1}{2}$ states, but the intermediate state is a mixed quantum state, a linear superposition of the two J states (Stenflo, 1980). The situation is fully analogous to the double-slit experiment, in which each photon has to pass through both slits at the same time, or to the Schrödinger cat, which is in a superposition of being both dead and alive. The level interference that results from this quantum superposition dramatically changes the intrinsic polarizabilities W_2 of the scattering system, in the same way as the interference pattern from a double slit is qualitatively different from an incoherent superposition of two single-slit interference patterns.

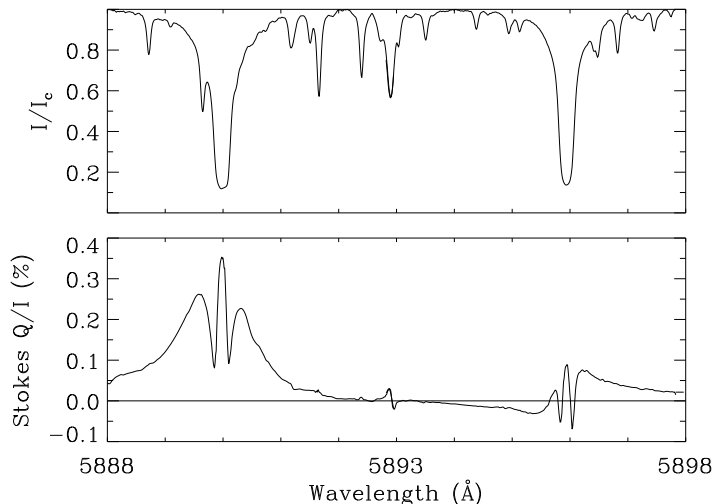


Fig. 5. Polarization structure from scattering at the sodium D₂ (5889.97 Å) and D₁ (5895.94 Å) system, as observed at 5 arcsec inside the limb of the quiet Sun (Stenflo *et al.*, 2000a). The polarization peak at the center of the D₁ line still remains an enigma.

As the next example we show the polarization in the D₂ and D₁ lines of neutral sodium (at 5889.97 and 5895.94 Å), from (Stenflo *et al.*, 2000a). These line transitions have the same J quantum number combinations as the K and H transitions that we have just discussed, but with an important difference: In contrast to calcium, sodium has a nuclear spin, $I = \frac{3}{2}$, which gives rise to a set of new levels with different combinations of total angular momentum quantum numbers F . However, even with these new quantum numbers the D₁ line at 5895.94 Å should remain intrinsically unpolarizable ($W_2 = 0$ at the center of the line). In contrast, the observations reveal a small but significant polarization peak centered around the D₁ resonance.

Another mechanism that has considerable influence on the intrinsic line polarizability is polarization transfer by optical pumping, as suggested by Landi Degl’Innocenti (1998, 1999). The atomic polarization of the excited state that is induced by the anisotropic illumination is partially transferred and mapped into the otherwise unpolarized ground state through the spontaneous emission process. After many scattering processes a statistical equilibrium is reached, in which the ground state possesses atomic polarization. Scattering from a polarized ground state can produce greatly different scattering polarization as compared with scattering from an unpolarized state.

While such optical pumping has been found to play a decisive role in certain atomic multiplets (cf. Sect. 5 below), it is insufficient for explaining the observed D₂ – D₁ polarization, since the observed polarization amplitude is 1-2 orders of magnitude larger and the symmetry opposite to the theoretical prediction (Trujillo Bueno *et al.*, 2002; Kerkeni & Bommier, 2002; Casini *et al.*, 2002; Klement & Stenflo, 2003; Casini & Manso Sainz, 2005). The origin of this discrepancy has not yet been identified. To clarify the

underlying physics we have therefore set up a laboratory experiment at ETH Zurich to study the polarizing properties of scattering at potassium vapor (Thalmann *et al.*, 2006). Potassium has the same quantum structure as sodium and has been chosen for the experiment, since solid-state tunable lasers are available for the potassium wavelengths, in contrast to the wavelengths of the sodium lines. The experiment is still in progress.

4. Unique role of eclipse observations

We have seen in the previous sections that the observed scattering polarization on the Sun is much smaller than the values of the Chandrasekhar solution, but that the observed center-to-limb variation is much steeper. In the Chandrasekhar solution the opacity is determined exclusively by polarizing dipole-type scattering at all heights in the atmosphere, while on the real Sun scattering becomes insignificant deep in the atmosphere, where the collisional rates dominate over the radiative rates. As we go up in the atmosphere the density and therefore also the collision rates decrease until the radiative rates take over. Therefore the polarizing scattering layer lies systematically above the non-polarizing opacity layers. As we approach the limb we sample increasingly higher layers of the atmosphere, where polarizing scattering plays an increasingly significant role. At the top of the atmosphere, corresponding to the extreme limb where $\mu = 0$, it should be possible to disregard collisions entirely, which implies that we approach conditions that are much more similar to the pure scattering case considered by Chandrasekhar.

It should be noted, however, that this does not imply that the Chandrasekhar solution should be asymptotically reached in quantitative detail. Even if the top layer were governed exclusively by scattering processes, and even if the scattering particles would have intrinsic polarizability $W_2 = 1$ (like classical scattering), the polarization at the extreme limb would still differ from the Chandrasekhar case. The main reason is that the solar limb darkening, which determines the anisotropy of the radiation field that illuminates the scattering layer, is governed by non-local processes in deeper layers that are not dominated by scattering, in contrast to the idealized atmosphere governed by scattering at all heights. Still there is reason to expect that there should be a dramatic enhancement of the polarization amplitude within the last couple of arcsec of the extreme limb, such that polarization amplitudes in some spectral lines would asymptotically reach magnitudes comparable to the Chandrasekhar limit of 11.7%. To deepen our general understanding of the formation of stellar spectra it would be of great interest to explore how the scattering polarization varies at the extreme limb in different parts of the spectrum, both through theoretical modelling and through observations. Neither has been done so far.

The reason why the polarization at the extreme limb has not been explored before is that one really needs a total solar eclipse to do it well. The window of opportunity occurs only during the flash phase, during the brief but dramatic transition between the partial and total phase at second and third contact of the eclipse sequence. The limb of the Moon serves as a knife edge that successively covers the different height layers of the Sun's atmosphere. Since the spectral intensity drops steeply with height, the contribution to the flash spectrum is dominated by the atmospheric layer that lies immediately adjacent to the Moon's limb. As the Moon moves about $\frac{1}{2}$ arcsec per second, we would obtain the phenomenal height resolution of order 10 km if we use a frame rate of 50 frames/s, which is the nominal choice for our 29 March 2006 eclipse experiment (Feller *et al.*, 2006).

The two main obstacles preventing good recordings of the extreme limb polarization outside an eclipse are (1) spatial resolution, and (2) stray light. The best spatial resolution that can currently be achieved corresponds to about 100 km on the Sun, or an order of magnitude worse in height resolution than the eclipse would offer. The difference is

actually much larger than this, since 100 km resolution has never been reached in combination with sensitive polarimetry, and much less in combination with large spectral coverage (our eclipse experiment has a simultaneous spectral coverage of about 5000 Å, cf. Feller *et al.*, 2006). These limitations are equally valid for both ground-based and space-based instruments. While the behavior of the spectral distribution of the scattering polarization (the “Second Solar Spectrum”) has been extensively explored during the past decade for disk positions up to 5 arcsec inside the Sun’s limb, it is the dramatic polarization increase within the last couple of arcsec that has not yet been captured, and for this we need a solar eclipse.

Due to the steep intensity drop at the extreme limb, small amounts of stray light in the instrument or in the Earth’s atmosphere may seriously contaminate the observations. Instrumental stray light may be suppressed by a coronagraphic design, using an occulting disk to produce an artificial eclipse. However, scattering from the illuminated bright edge of the occulting disk will be a serious source of stray light (in addition to scattering at microscopic inhomogeneities in the optical components). Using optical tricks like the Lyot design with a field lens, the scattered light from the edge of the occulting disk can be significantly suppressed but not eliminated. The remaining stray light would still cause serious contamination. Note that in ordinary coronagraphs the occulting disk is significantly larger than the solar disk (in space coronagraphs like LASCO it is much larger), so that the edge of the occulting disk is not directly exposed to the solar disk. To isolate the different height layers at the extreme limb, however, the edge of the occulting disk has to be a fraction of an arcsec *inside* the limb and be shifted progressively outwards. The edge is therefore directly exposed to the bright disk, which makes the stray light problem much more serious than in standard coronagraphs. Note also that the telescopes that currently reach the best spatial resolution, approaching 100 km, do not have a coronagraphic design.

A method to remove most of the effects of image motions due to atmospheric seeing and thereby achieve a higher limb and μ resolution has been developed and implemented by Sheeley & Keller (2003) by recording a large number of frames with high time resolution and then using the intensity level of each frame to assign a μ value and organize the frames in μ bins. While this rather laborious method removes much of the seeing smearing due to image motions (without the use of adaptive optics), the limitations of stray light and telescope resolution are not overcome.

At an eclipse the Moon is our occulting disk. In contrast to artificial occulting disks both the spatial resolution and stray light limitations are entirely eliminated when the Moon is used. The reason why the spatial resolution problem is eliminated is that the exact position of the Moon’s edge is fixed with respect to the Sun (for each given moment of time), entirely independent of any seeing, image motion, telescope pointing or resolution. The reason why stray light from the lunar occulting disk is completely irrelevant is because the Moon is so far away, so that the solid angle occupied by the telescope aperture as seen from the Moon is vanishingly small. An artificial occulting disk in or near the telescope on the other hand will scatter into the instrument over a large solid angle.

The main imperfection of the Moon’s edge as our knife edge is that it is not straight but somewhat jagged due to the lunar craters and valleys. This causes the Moon’s limb to wiggle up and down by an amount that on the Sun may correspond to a few tens of km, depending on which part of the Moon’s limb is used. With modest spatial resolution in the direction along the Moon’s limb one may easily resolve these wiggles and account for them in the analysis, thereby avoiding significant reduction of the height resolution. Still the jaggedness of the Moon’s limb will cause some moderate degradation, since local stray light from the brighter valleys may contaminate the fainter hills along the Moon’s limb.

5. Differential effects in the polarized flash spectrum

We have seen in Sects. 2 and 3 that the polarized spectrum is highly structured and the expected polarization effects are very different in different spectral lines. The various line transitions have individual intrinsic physical properties and respond very differently to the atmospheric structure. These differential effects contain potentially rich diagnostic information about the solar atmosphere and the physics of line formation, but they also provide crucial help in the removal of instrumental effects in the data reduction process. In contrast the idealized Chandrasekhar solution has a universal center-to-limb variation without any spectral structures.

One of the notoriously most difficult problems in high-precision polarimetry is the determination of the true zero point of the polarization scale. The *absolute* polarization amplitudes generally cannot be determined with accuracies comparable to those of the *relative* amplitudes. When comparing two spectra in orthogonal polarization states, placed side by side (via a polarizing beam splitter), or recorded one after the other (via polarization modulation), their intensities will differ if polarization is present, but they may also differ for other reasons (imbalance of the beam splitter and of the detector gain table, or asymmetries in the modulation). These other effects will generate a fictitious polarization signal, usually in the form of an offset of the zero point of the polarization scale. To fix the zero point we need to lock it to some spectral feature for which we can assume that its intrinsic polarization must be zero or at least small in comparison with other spectral structures.

One example of a spectral feature with intrinsically zero polarization is the Ca II H line at 3968 Å, as we saw in Fig. 4. By locking the zero point of the polarization scale to this line and differentially relate the apparent Ca II K polarization to that of the H line, we can obtain the true, absolute value of the K polarization from the relative scale.

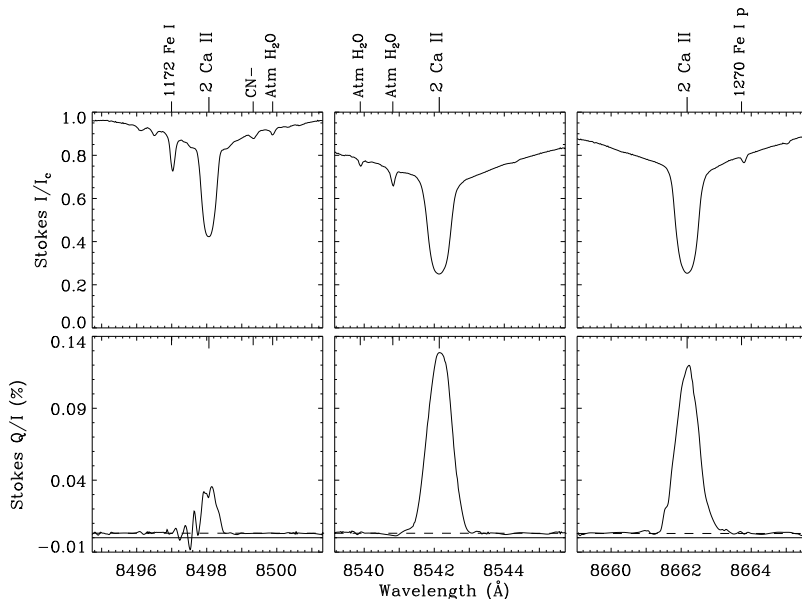


Fig. 6. Scattering polarization from the Ca II infrared triplet, as recorded at $\mu = 0.1$ (5 arcsec inside the solar limb) on the quiet Sun, from Stenflo *et al.* (2000b). The relative polarization amplitudes have been found to be governed by optical pumping (Manso Sainz & Trujillo Bueno, 2003).

This differential procedure works best when comparing the relative polarization amplitudes for lines that belong to the same atomic multiplet and have different intrinsic polarizabilities, like the K and H line multiplet, or the sodium D₂ and D₁ multiplet (both of which only contain these two lines). Another very useful case is that of the

Ca II infrared triplet at 8498, 8542, and 8662 Å, which is shown in Fig. 6, from Stenflo *et al.* (2000b). This multiplet has the same upper levels as the K and H line multiplet, but has different lower states. It can therefore be fluorescently coupled to the K and H lines (radiative excitation in the ultraviolet, emission in the infrared).

According to the J quantum numbers of the transitions, the intrinsic polarizabilities W_2 would be expected to be zero for the 8662 Å line of the infrared triplet, while the 8498 Å line should be the most polarizable. The observed amplitude relations in Fig. 6 are however qualitatively entirely different, with the 8498 Å line exhibiting much less polarization than the 8662 Å line. An explanation for this behavior has been found in terms of optical pumping (Manso Sainz & Trujillo Bueno, 2003). The radiatively induced atomic polarization in the excited $J = \frac{3}{2}$ state is partially transferred to the lower states by the spontaneous emission process, until, after many such scattering processes, a statistical equilibrium is reached. Scattering from initially polarized lower states produces scattering polarization that is very different from the values expected from W_2 alone.

Since the optical pumping process is not a function of center-to-limb distance, one may use the observed ratios between the polarization amplitudes in the three lines as representative for the intrinsic ratios in the flash spectrum, and adopt this as a constraint to fix the location of the true zero point of the polarization scale in this infrared portion of the spectrum.

Another independent constraint on the true zero point is the qualitatively known approximate shape of the center-to-limb variation of the polarization: We know from previous, non-eclipse observations that the polarization drops to values usually well below 1% already a few arcsec inside the solar limb, and then continues to drop in a rather well defined way (cf. Fig. 3). The level of the zero point of the polarization scale has to be consistent with this observed fact.

6. Concluding remarks

With observations from space of the Sun's corona in EUV and X-rays, or with coronagraphs in the visible, the special circumstances offered by a total solar eclipse may appear to be less unique and scientifically attractive than they used to be in the past. There is however one scientific measurement that cannot be accomplished well without a total solar eclipse, namely the determination of the polarization of the flash spectrum. Such a measurement would give us the scattering polarization near the extreme limb of the Sun, as it is formed in the different height layers of the solar atmosphere. The Moon's limb serves as a knife edge that moves across the different height layers, covering them up or uncovering them in a well-defined way that is free from effects of seeing, telescope resolution, and stray light. The polarization of the flash spectrum is expected to have a structural richness that contains novel diagnostic information on the conditions in the solar atmosphere and on the physics of spectral line formation. Still the polarization of the flash spectrum has never been recorded with any success in the past.

The Chandrasekhar solution for an idealized, purely scattering atmosphere with a plane-parallel stratification exhibits very high polarization values, reaching the asymptotic value of 11.7% at the extreme limb. Observations of the scattering polarization 5 arcsec or more inside the limb show much smaller values, generally much below 1%, and the polarized spectrum is found to be extremely structured (and is therefore called the "Second Solar Spectrum"), in contrast to the Chandrasekhar solution. The main reason for this difference is that collisional effects and non-scattering opacities dominate in much of the solar photosphere. As we move up in the atmosphere, however, the collision rates decrease to become smaller than the radiative rates due to the drop in density with height. Scattering then plays an increasing role relative to true absorption. This

implies that we approach conditions that are more similar to the idealized conditions that are assumed in the Chandrasekhar solution as we move up into the chromosphere. The steep increase in polarization that we already observe at a limb distance of 5 arcsec may therefore dramatically increase within the last arcseconds from the limb to possibly become comparable to the Chandrasekhar values. Whether this is really the case or not has never been explored before, but it needs a total solar eclipse to be empirically addressed.

During the flash phase, which has a duration of order 20 s, the Sun's spectrum changes dramatically from an absorption-line spectrum that originates in the photosphere to an emission-line spectrum that comes from the chromosphere. The precise location of the Sun's limb depends on wavelength and type of spectrum. The emission lines naturally originate above the photospheric limb. Therefore the translation of position into center-to-limb distance or μ becomes ambiguous and loses its meaning at the extreme limb or above.

While the assumption of a plane-parallel stratification has often worked well for modelling of the photosphere, it loses its validity when the line-of-sight has almost grazing incidence near the extreme limb, and due to the Sun's spherical geometry the horizontal optical thickness becomes finite instead of the semi-infinite plane-parallel stratification. The transition from the photosphere to the chromosphere is not only a transition from an absorption-line to an emission-line spectrum, but also a transition to a force-free, magnetically controlled plasma that is highly filamentary and dynamic, with large local fluctuations of the thermodynamic parameters. The resulting local fluctuations in the radiation-field anisotropy will affect the local values of the scattering polarization. Randomly oriented small-scale magnetic fields may cause depolarization via the Hanle effect. Realistic theoretical modelling of these effects is a difficult undertaking that still has to be done, but it needs observational guidance.

Ideally the observations during the flash phase should combine high polarimetric sensitivity with broad spectral coverage and high temporal, spectral, and spatial resolution. In the past nobody has ever recorded the flash spectrum successfully with high polarimetric sensitivity even without any of the other resolutions or spectral coverage. In our experiment for the 29 March 2006 eclipse at Waw an Namos we aim to record the flash spectrum with reasonably high polarimetric accuracy (promille range), large spectral coverage and high temporal resolution, but with modest spectral and spatial resolutions. It is a good beginning, but we have a long way to go. Improved generations of the experiment at future total solar eclipses will be needed to asymptotically approach the ideal of a perfectly resolved polarized flash spectrum.

References

- Casini, R., Manso Sainz, R.: 2005, *ApJ*, **624**, 1025
 Casini, R., Landi Degl'Innocenti, E., Landolfi, M., Trujillo Bueno, J.: 2002, *ApJ*, **573**, 864
 Chandrasekhar, S.: 1950, *Radiative Transfer*, Clarendon Press, Oxford
 Feller, A., Stenflo, J.O., Gisler, D., Ramelli, R.: 2006, these proceedings
 Fluri, D.M., Stenflo, J.O.: 1999, *A&A*, **341**, 902
 Gandorfer, A.: 2000, *The Second Solar Spectrum, Vol. I: 4625 Å to 6995 Å*, ISBN no. 3 7281 2764 7 (Zurich: VdF)
 Gandorfer, A.: 2002, *The Second Solar Spectrum, Vol. II: 3910 Å to 4630 Å*, ISBN no. 3 7281 2855 4 (Zurich: VdF)
 Gandorfer, A.: 2005, *The Second Solar Spectrum, Vol. III: 3160 Å to 3915 Å*, ISBN no. 3 7281 3018 4 (Zurich: VdF)
 Kerkeni, B., Bommier, V.: 2002, *A&A*, **394**, 707
 Klement, J., Stenflo, J.O.: 2003, in J. Trujillo Bueno and J. Sánchez Almeida (Eds.), *Solar Polarization*, Proc. 3rd SPW, *ASP Conf. Ser.*, **307**, 278
 Landi Degl'Innocenti, E.: 1998, *Nature*, **392**, 256
 Landi Degl'Innocenti, E.: 1999, in K.N. Nagendra and J.O. Stenflo (Eds.), *Solar Polarization*, Proc. 2nd SPW, *Astrophys. Space Sci. Library*, **243**, 61 (Dordrecht: Kluwer)
 Manso Sainz, R., Trujillo Bueno, J.: 2003, *Phys. Rev. Lett.* **91**, 111102

JAN O. STENFLO

- Sheeley, N.R., Jr., Keller, C.U.: 2003, *ApJ*, **594**, 1085
Stenflo, J.O.: 1980, *A&A*, **84**, 68
Stenflo, J.O.: 2004, *Rev. Mod. Astron.*, **17**, 269
Stenflo, J.O.: 2005, *A&A*, **429**, 713
Stenflo, J.O, Keller, C.U.: 1996, *Nature*, **382**, 588
Stenflo, J.O, Keller, C.U.: 1997, *A&A*, **321**, 927
Stenflo, J.O., Gandorfer, A., Keller, C.U.: 2000a, *A&A*, **355**, 781
Stenflo, J.O., Keller, C.U., Gandorfer, A.: 2000b, *A&A*, **355**, 789
Thalmann, C., Stenflo, J.O., Feller, A., Cacciani, A.: 2006, in R. Casini and B.W. Lites (Eds.), *Solar Polarization*, Proc. 4th SPW, *ASP Conf. Ser.*, in press
Trujillo Bueno, J., Casini, R., Landolfi, M., Landi Degl'Innocenti, E.: 2002, *ApJ*, **566**, L53